65. E. I. Rashba, *Phys. Rev. B* **62**, R16267 (2000).
66. M. E. Flatte, J. Byers, W. H. Hau, unpublished data.
67. L. C. Chen *et al.*, *J. Vac. Sci. Tech. B* **18**, 2057 (2000).
68. H. J. Zhu *et al.*, *Phys. Rev. Lett.* **87**, 016601 (2001).
69. G. Kirczenow, *Phys. Rev. B* **63**, 054422 (2001).
70. D. Grundler, *Phys. Rev. B* **63**, R161307 (2001).
71. S. K. Upadhyay *et al.*, *Phys. Rev. Lett.* **81**, 3247 (1998).
72. S. K. Upadhyay *et al.*, *Appl. Phys. Lett.* **74**, 3881 (1999).
73. D. Monsma *et al.*, *Phys. Rev. Lett.* **74**, 5260 (1995).
74. R. Jansen *et al.*, *J. Appl Phys.* **89**, 7431 (2001).
75. W. H. Rippard, R. A. Buhrman, *Phys. Rev. Lett.* **84**, 971 (2000).
76. H. X. Tang *et al.*, *Phys. Rev. B* **61**, 4437 (2000).
77. S. Datta, B. Das, *Appl. Phys. Lett.* **56**, 665 (1990).
78. L. J. Sham, T. Ostreich, *J. Lumin.* **87**, 179 (2000).
79. L. J. Sham, *J. Magn. Magn. Mat.* **200**, 219 (1999).
80. M. E. Flatte, G. Vignale, *Appl. Phys. Lett.* **78**, 1273 (2001).
81. L. Berger, *Phys. Rev. B* **54**, 9353 (1996).
82. J. C. Slonczewski, *J. Magn. Magn. Mater.* **159**, L1 (1996).
83. ———, *J. Magn. Magn. Mater.* **195**, L261 (1999).
84. M. Tsoi *et al.*, *Phys. Rev. Lett.* **80**, 4281 (1998) [erratum, *Phys. Rev. Lett.* **81**, 493 (1998)].
85. E. B. Myers, D. C. Ralph, J. A. Katine, R. N. Louie, R. A. Buhrman, *Science* **285**, 867 (1999).
86. S. M. Rezende *et al.*, *Phys. Rev. Lett.* **84**, 4212 (2000).
87. J. A. Katine *et al.*, *Phys. Rev. Lett.* **84**, 3149 (2000).
88. W. Weber, S. Riesen, H. C. Siegmann, *Science* **291**, 1015 (2001).
89. D. D. Awschalom, J. M. Kikkawa, *Phys. Today* **52**, 33 (1999).
90. J. M. Kikkawa, D. D. Awschalom, I. P. Smorchkova, N. Samarth, *Science* **277**, 1284 (1997).
91. J. M. Kikkawa, D. D. Awschalom, *Phys. Rev. Lett.* **80**, 4313 (1998).
92. ———, *Nature* **397**, 139 (1999).
93. J. A. Gupta, X. Peng, A. P. Alivisatos, D. D. Awschalom, *Phys. Rev. B* **59**, R10421 (1999).
94. M. Flatté, J. Byers, *Phys. Rev. Lett.* **84**, 4220 (2000).
95. Y. Ohno *et al.*, *Phys. Rev. Lett.* **83**, 4196 (1999).
96. I. Malajovich *et al.*, *Phys. Rev. Lett.* **84**, 1015 (2000).
97. I. Malajovich *et al.*, *Nature* **411**, 770 (2001).
98. B. Beschoten *et al.*, *Phys. Rev. B* **63**, R121202 (2001).
99. S. A. Crooker *et al.*, *Phys. Rev. Lett.* **75**, 505 (1995).
100. R. Fiederling *et al.*, *Nature* **402**, 787, (1999).
101. B. T. Jonker *et al.*, *Phys. Rev. B* **62**, 8180 (2000).
102. Y. Ohno *et al.*, *Nature* **402**, 790 (1999).
103. S. Koshihara *et al.*, *Phys. Rev. Lett.* **78**, 4617 (1997).
104. D. P. DiVincenzo *et al.*, *Nature* **408**, 339 (2000).
105. J. M. Kikkawa, D. D. Awschalom, *Science* **287**, 473 (2000).
106. G. Salis *et al.*, *Phys. Rev. Lett.* **86**, 2677 (2001).
107. R. K. Kawakami *et al.*, *Science* **294**, 131 (2001).
108. D. Loss, D. P. DiVincenzo, *Phys. Rev. A* **57**, 120 (1998).
109. G. Burkard, H. Engel, D. Loss, *Fortschr. Phys.* **48**, 965 (2000).
110. H.-A. Engel, D. Loss, *Phys. Rev. Lett.* **86**, 4648 (2001).
111. A. Imamoglu *et al.*, *Phys. Rev. Lett.* **83**, 4204, (1999).
112. N. H. Bonadeo *et al.*, *Science* **282**, 1473 (1998).
113. N. Paillard *et al.*, *Phys. Rev. Lett.* **86**, 1634 (2001).
114. J. A. Gupta *et al.*, *Science* **292**, 2458 (2001).
115. B. Kane, *Nature* **393**, 133 (1998).
116. R. Vrijen *et al.*, *Phys. Rev. A* **62**, 012306, (2000).
117. J. P. Gordon, *Phys. Rev. Lett.* **1**, 368 (1958).
118. M. A. Korotini *et al.*, *Phys. Rev. Lett.* **80**, 4305 (1998).
119. S. Watts, private communication.
120. J. M. Kikkawa *et al.*, *Physica E* **9**, 194 (2001).

121. This article was motivated in part from a WTEC study on Spin Electronics sponsored by the Defense Advanced Research Projects Agency, the NSF, Office of the Secretary of Defense, and National Institute of Standards and Technology.

REVIEW

Spin Ice State in Frustrated Magnetic Pyrochlore Materials

Steven T. Bramwell[1] and Michel J. P. Gingras[2,3]*

A frustrated system is one whose symmetry precludes the possibility that every pairwise interaction ("bond") in the system can be satisfied at the same time. Such systems are common in all areas of physical and biological science. In the most extreme cases, they can have a disordered ground state with "macroscopic" degeneracy; that is, one that comprises a huge number of equivalent states of the same energy. Pauling's description of the low-temperature proton disorder in water ice was perhaps the first recognition of this phenomenon and remains the paradigm. In recent years, a new class of magnetic substance has been characterized, in which the disorder of the magnetic moments at low temperatures is precisely analogous to the proton disorder in water ice. These substances, known as spin ice materials, are perhaps the "cleanest" examples of such highly frustrated systems yet discovered. They offer an unparalleled opportunity for the study of frustration in magnetic systems at both an experimental and a theoretical level. This article describes the essential physics of spin ice, as it is currently understood, and identifies new avenues for future research on related materials and models.

Competing or frustrated interactions are a common feature of condensed matter systems. Broadly speaking, frustration arises when a system cannot, because of local geometric constraints, minimize all the pairwise interactions simultaneously (*1*). In some cases, the frustration can be so intense that it induces novel and complex phenomena. Frustration is at the origin of the intricate structure of molecular crystals, various phase transitions in liquid crystals, and the magnetic domain structures in ferromagnetic films. It has also been argued to be involved in the formation of the stripelike structures observed in cuprate high-temperature superconductors. The concept of frustration is a broad one that extends beyond the field of condensed matter physics. For example, the ability of naturally occurring systems to "resolve" frustrated interactions has been argued to have bearings on life itself, exemplified by the folding of a protein to form a single and well-prescribed structure with biological functionality.

[1]Department of Chemistry, University College London, 20 Gordon Street, London WC1H 0AJ, UK. [2]Department of Physics, University of Waterloo, Waterloo, Ontario, N2L-3G1, Canada. [3]Canadian Institute for Advanced Research, 180 Dundas Street, Toronto, Ontario M5G 1Z8, Canada.

*To whom correspondence should be addressed. E-mail: gingras@gandalf.uwaterloo.ca.

Historically, the first frustrated system identified was crystalline ice, which has frozen-in disorder remaining down to extremely low temperature, a property known as residual, or zero-point entropy. In 1933, Giauque and co-workers accurately measured this entropy (*2*, *3*), enabling Pauling to offer his now famous explanation in terms of the mismatch between the crystal symmetry and the local bonding requirements of the water molecule (*4*). He predicted a special type of proton disorder that obeys the so-called "ice rules." These rules, previously proposed by Bernal and Fowler (*5*), require that two protons are near to and two are further away from each oxide ion, such that the crystal structure consists of hydrogen-bonded water molecules, H_2O (see Fig. 1). Pauling showed that the ice rules do not lead to order in the proton arrangement but rather, the ice ground state is "macroscopically degenerate." That is to say, the number of degenerate, or energetically equivalent proton arrangements diverges exponentially with the size of the sample. Pauling estimated the degeneracy to be $\sim(3/2)^{N/2}$, where N is the number of water molecules, typically $\sim 10^{24}$ in a macroscopic sample. This leads to a disordered ground state with a measurable zero-point entropy S_0 related to the degeneracy: $S_0 \approx (R/2)\ln(3/2)$, where R is the molar gas constant. Pauling's estimate of S_0 is very close to the most accurate modern estimate (*6*) and consistent with experiment (*2*). The disordered ice–rules proton arrangement in water ice was eventually

confirmed by neutron diffraction experiments (*7*, *8*).

Magnetic systems offer themselves as the ideal benchmark for generic concepts pertaining to collective phenomena in nature. This is due in part to the availability of a large variety of diverse magnetic materials that can be chosen to approximate simple theoretical "toy models" of collective behavior and, in part, to their ease of study by a battery of experimental techniques. Over the last 50 years, experimentalists have characterized new classes of frustrated magnetic behavior, and theoreticians have been motivated by the broad conceptual applicability of magnetic models to investigate simple frustrated spin systems (*9*–*11*). These include "energetic" generalizations of the ice model that display a wealth of interesting thermodynamic phenomena in close resemblance with those observed in real ice (*12*, *13*). However, although theoretical studies of ice-like phenomena in frustrated ice models have long flourished, very few, if any, real magnets could be found to display a close thermodynamic resemblance to common ice. This remained for some time a disappointing situation where close contact between theoretical studies on magnetic ice models and real systems was lacking, a somewhat untenable predicament in science where one is generally aiming at testing theoretical concepts against experiments and vice versa.

Anderson had noticed in 1956 the formal analogy that exists between the statistical mechanics of cation ordering on the cubic B-site lattice in "inverse" spinel materials and the statistical mechanics of antiferromagnetically coupled two-state Ising magnetic moments on the same lattice (referred to here as the pyrochlore lattice, Fig. 1C) (*14*). Both systems were shown to map exactly onto Pauling's model of proton disorder in ice. The realization of Anderson's model in an antiferromagnetic material would require spins to point along or antiparallel to a global *z*-axis direction. However, there is no reason to prefer the *z* over the *x* or the *y* direction in a lattice with global cubic symmetry, and this renders the global antiferromagnetic Ising model unrealistic with no direct relation to any real magnetic material. The experimental situation changed in 1997, when it was noticed by Harris *et al.* (*15*) that a model of ferromagnetism on the pyrochlore lattice would exactly map onto the ice model so long as each Ising-like magnetic moment was constrained to point along the axis joining the centers of the two tetrahedra to which it belongs (Fig. 1C). This was a surprising observation, because naïvely one would not expect frustration in a ferromagnet. However, the ferromagnetic model is compatible with cubic symmetry and was observed to be approximated by the apparently ferromagnetic pyrochlore material $Ho_2Ti_2O_7$ (*15*). This constituted the first simple physical realization of a real three-dimensional magnetic analog of common ice, and the name "spin ice" was coined to emphasize this analogy.

Experiments on spin ice have mirrored, using modern sophistication, those originally conducted on water ice. However, the spin ice materials lend themselves more readily to experiment than does water ice and more closely approximate tractable theoretical models. This has led to much recent interest devoted to the problem of zero-point entropy and to the study of the broad consequences of geometric frustration. We review the recent experimental and theoretical developments in the study of spin ice materials, and discuss what are possible new and exciting avenues of research in this problem.

Discovery of Spin Ice

In a flux-grown crystal of $Ho_2Ti_2O_7$ (*16*) (Fig. 2) the octahedral habit reflects the cubic symmetry of the pyrochlore structure; the amber color and strong reflectivity are indicative of a band gap near the visible/ultraviolet boundary (3.2 eV). In $Ho_2Ti_2O_7$, the Ho^{3+} ions occupy a pyrochlore lattice of corner-linked tetrahedra (illustrated in Fig. 1C). Magnetism arises from the Ho^{3+} ions, as Ti^{4+} is nonmagnetic. Ho^{3+} has a particularly large magnetic moment of approximately $10\mu_B$ that persists to the lowest temperatures and makes the crystals sufficiently paramagnetic to stick to a permanent magnet even at room temperature (Fig. 2). The large, temperature-independent moment is ensured by the local crystallographic environment of Ho^{3+} in the pyrochlore structure (*17*–*21*). Each tetrahedron of Ho^{3+} ions has an oxide ion at its center, so two of these oxide ions lie close to each Ho^{3+} along the ⟨111⟩ crystallographic axis that connects the center of the tetrahedron to its vertex. The anisotropic crystallographic environment changes the quantum ground state of Ho^{3+} such that its magnetic moment vector has its maximum possible magnitude and lies parallel to the local ⟨111⟩ axis. In the language of quantum mechanics the ${}^5I_8$ free ion state is split by the local trigonal crystal field such that the ground state is an almost pure $|J, M_J\rangle = |8, \pm 8\rangle$ doublet with ⟨111⟩ quantization axis. The first excited state lies several hundreds of Kelvin above the ground state as revealed by inelastic neutron-scattering measurements (*21*). At temperatures on the order of 10 K or below,

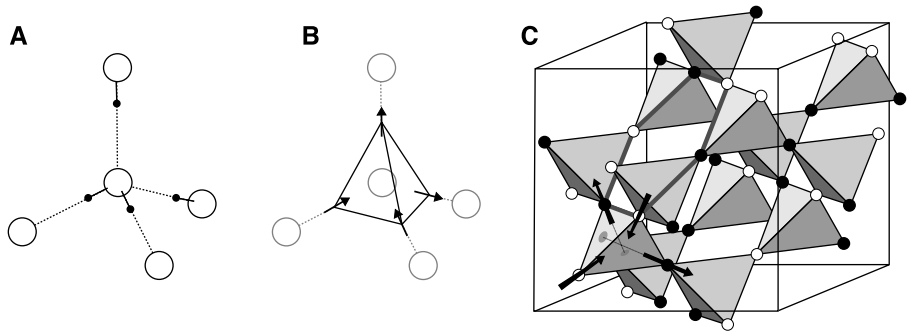

Fig. 1. (**A**) Local proton arrangement in water ice, showing oxide ions (large white circles) and protons (hydrogen ions, small black circles). Each oxide is tetrahedrally coordinated with four other oxides, with two near covalently bonded protons, and two are further hydrogen-bonded protons. The low-energy configurations obey the so-called "ice rules" (*5*), where each oxide has two "near" and two "far" protons. (**B**) Same as in (A), but where now the position of the protons are represented by displacement vectors (arrows) located at the midpoints of the oxide-oxide lines of contact. The ice rules in (A) translates into a two-in, two-out configuration of the displacement vectors. (**C**) Pyrochlore lattice of corner-sharing tetrahedra, as occupied by the magnetic rare-earth ions in the spin ice materials $Ho_2Ti_2O_7$ and $Dy_2Ti_2O_7$. The magnetic Ising moments occupy the corners of the tetrahedra, as shown on the lower left "downward" tetrahedron of the lattice (arrows). The spins here are the equivalents of the proton displacement vectors in (B). Each spin axis is along the local ⟨111⟩ quantization axis, which goes from one site to the middle of the opposing triangular face (as shown by the disks) and meets with the three other ⟨111⟩ axes in the middle of the tetrahedron. In the spin ice materials the two-in, two-out condition arises from the combined effect of magnetic coupling and anisotropy. For clarity, other spins on the lattice are denoted by black and white circles, where white represents a spin pointing into a downward tetrahedron; black is the opposite. The entire lattice is shown in an ice-rules state (two black and two white sites for every tetrahedron). The hexagon (thick gray line) relates to the discussion in the section on open issues and avenues for future advances. It shows the smallest possible loop move involving multiple spins, and corresponds to reversing all colors (spins) on the loop to produce a new ice-rules state. These extended type of excitations or processes are the ones that allow the system to explore the quasi-degenerate ice rule manifold at low temperature. Common water ice at atmospheric pressure, ice I_h, has a hexagonal structure, whereas here, the magnetic lattice has cubic symmetry. Strictly speaking, the Ising pyrochlore problem is equivalent to cubic ice, and not the hexagonal phase. Yet, this does not modify the ice-rule analogy (or mapping) or the connection between the statistical mechanics of the local proton coordination in water ice and the low-temperature spin structure of the spin ice materials.

the excited states are not accessed thermally. The Ho^{3+} moments therefore behave as almost pure two-state spins that approximate classical Ising spins pointing "in" or "out" of the elementary tetrahedra (Fig. 1). Direct evidence of the single ion anisotropy comes from bulk magnetization (*18*, *19*, *22*), where saturation is observed at roughly half the expected value, owing to the fact that applied fields of several Tesla are too weak to turn the Ho^{3+} significantly away from their local quantization axes.

Experimental investigation of the spin correlations in $Ho_2Ti_2O_7$ began in 1996 (*15*). Before this, susceptibility measurements (*24*) had revealed a peak in the susceptibility of $Ho_2Ti_2O_7$ at ≈1 K, suggestive of antiferromagnetic interactions. The first muon spin relaxation (μSR) and neutron-scattering experiments seemed to confirm this frustrated antiferromagnetic scenario with no evidence of long-range order down to ~50 mK (*15*, *23*). However, a pyrochlore antiferromagnet, with essentially infinite local ⟨111⟩ Ising anisotropy, should develop a long-range ordered state at a critical temperature of order of the Curie-Weiss temperature (θ_{CW}), ≈1 K (*25*, *26*). Consequently, the failure of $Ho_2Ti_2O_7$ to display a transition down to ≈50 mK was found to be rather paradoxical. However, new susceptibility studies soon suggested a rather different picture. The large moment of Ho^{3+} was found to produce a strong demagnetizing field that caused the experimental Curie-Weiss temperature (measured by the intercept of the inverse susceptibility versus temperature curve) to be either ferromagnetic or antiferromagnetic depending on crystal shape. Careful correction for this shape-dependent effect indicated that $\theta_{CW} = 1.9 \pm 0.1$ K, an intrinsically ferromagnetic value. It therefore seemed that $Ho_2Ti_2O_7$ should be described, at least to a first approximation, as a ⟨111⟩ Ising ferromagnet. But this description at first seemed contrary to the observed absence of long-range order—it was "obvious" that a ferromagnet should order at low temperature!

As often happens in science, the paradox was resolved as soon as the obvious was abandoned in the face of experimental evidence.

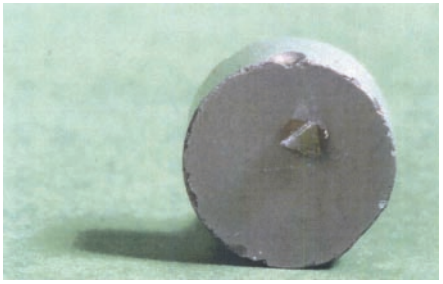

Fig. 2. Flux-grown octahedral crystal of $Ho_2Ti_2O_7$ stuck to a NdFeB permanent magnet at room temperature. The strong paramagnetism reflects the large magnetic moment of Ho^{3+}.

Calculation showed that the ground state of a tetrahedron of ferromagnetically coupled Ising spins is the "two-in, two-out" state illustrated in Fig. 1. It was then recalled that Anderson had shown the pyrochlore lattice to be the medial lattice (lattice formed by the midpoints of the bonds) of the diamond-like oxide lattice of cubic ice (*14*). Hence, the two-in, two-out condition is analogous to the ice rules, and the ground state of the nearest-neighbor ferromagnetic model is, like that of ice, macroscopically degenerate (*15*, *25*). The absence of long-range order in $Ho_2Ti_2O_7$ could then be explained at a qualitative level and the "spin ice" model, the ⟨111⟩ Ising ferromagnet, was christened. This simple model was found to be consistent with the field-induced ordering patterns observed by neutron scattering (*15*). On the basis of similar susceptibility properties, $Dy_2Ti_2O_7$ and $Yb_2Ti_2O_7$ were also suggested to be spin ice materials (*27*). So far, only $Ho_2Ti_2O_7$ (*15*, *28*), $Dy_2Ti_2O_7$ (*29*, *30*), and, more recently, $Ho_2Sn_2O_7$ (*31*), have been positively confirmed.

The magnetization and elastic neutron-scattering measurements described above provided the initial compelling arguments for the spin ice phenomenology associated with $Ho_2Ti_2O_7$ (*15*). However, specific-heat measurements by Ramirez and co-workers (*29*, *32*) on $Dy_2Ti_2O_7$ have given a more direct experimental evidence of the macroscopic degeneracy associated with the spin-ice rules. The top panel of Fig. 3 shows the temperature dependence of the magnetic specific heat, $C(T)$, for a powdered sample of $Dy_2Ti_2O_7$ (*29*). The data show no sign of a phase transition, as would be indicated by a sharp feature in $C(T)$. Instead, one observes a broad maximum at a temperature $T_{peak} = 1.2$ K,

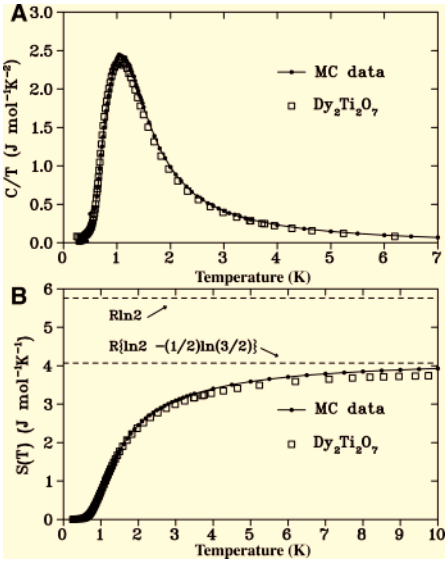

Fig. 3. (**A**) Specific-heat and (**B**) entropy data for $Dy_2Ti_2O_7$ (*29*) compared with Monte Carlo simulation results for the dipolar spin ice model (*34*), with $J_{nn} = -1.24$ K, $D_{nn} = 2.35$ K and system size of 1024 spins.

which is on the order of the energy scale of the magnetic interactions in that material, as measured by the Curie-Weiss temperature, ≈1 K. The specific heat has the appearance of a Schottky anomaly, the characteristic curve for a system with two energy levels. At the low-temperature side of the Schottky peak, $C(T)$ falls rapidly toward zero, indicating an almost complete freezing of the magnetic moments.

Ramirez and colleagues determined the ground-state entropy using a method analogous to that applied by Giauque and co-workers to water ice. In general one can only measure a change in entropy between two temperatures. Giauque *et al.* computed the entropy change of water between liquid helium temperatures and the gas phase by integrating the specific heat (*2*) and then comparing this value with the absolute entropy calculated for the gas phase using spectroscopic measurements of the energy levels of the water molecule. The difference gave the residual entropy, later calculated by Pauling (*4*). The approach of Ramirez and co-workers was to integrate the magnetic specific heat between $T_1 = 300$ mK in the frozen regime and $T_2 = 10$ K in the paramagnetic regime, where the expected entropy should be $R\ln(2)$ for a two-state system. The magnetic entropy change, ΔS, was determined by integrating $C(T)/T$ between these two temperatures:

$$\Delta S_{1,2} = \int_{T_1}^{T_2} \frac{C(T)}{T}\, dT \qquad (1)$$

The lower panel of Fig. 3 shows that the magnetic entropy recovered is about 3.9 J mol^{-1} K^{-1}, a number that falls considerably short of the value $R\ln(2) \approx 5.76$ J mol^{-1} K^{-1}. The difference, 1.86 J mol^{-1} K^{-1} is quite close to Pauling's estimate for the entropy associated with the extensive degeneracy of ice: $(R/2)\ln(3/2) = 1.68$ J mol^{-1} K^{-1}, consistent with the existence of an ice-rule obeying spin ice state in $Dy_2Ti_2O_7$.

Dipolar Spin Ice

As mentioned above, the magnetic cations Ho^{3+} and Dy^{3+} in $Ho_2Ti_2O_7$ and $Dy_2Ti_2O_7$ carry a very large magnetic moment, μ, of about $10\mu_B$. Furthermore, these moments are exceedingly well characterized by almost perfect effective classical Ising spins constrained to point along the local ⟨111⟩ directions below a temperature on the order of 200 K for $Ho_2Ti_2O_7$ and 300 K for $Dy_2Ti_2O_7$. This is borne out from direct experimental evidence (see Fig. 2), magnetization measurements, inelastic neutron measurements, and crystal field theoretical calculations (*17*–*21*). Large magnetic moments are reasonably common among rare-earth materials, and this gives rise to a sizable magnetic dipole energy. With a cubic unit cell dimension $a \approx 10.1$ Å, an estimate of the dipolar energy scale for two ⟨111⟩ Ising moments, D_{nn}, gives

$$D_{nn} = \frac{5}{3}\left(\frac{\mu_0}{4\pi}\right)\frac{\mu^2}{r_{nn}^3} = +2.4\ \text{K} \qquad (2)$$

where $r_{nn} = (a/4)\sqrt{(2)}$ is the nearest-neighbor distance. As discussed below, the 5/3 factor originates from the orientation of the Ising quantization axes relative to the vector direction connecting nearest-neighbor magnetic moments. The experimentally determined Curie-Weiss temperature, θ_{CW}, extrapolated from temperatures below $T \sim 100$ K is $\theta_{CW} \approx +1.9$ K for $Ho_2Ti_2O_7$ (*15*) and +0.5 K for $Dy_2Ti_2O_7$ (*29*), respectively. These two values show that θ_{CW} is of the same order of magnitude as the nearest-neighbor dipolar energy scale D_{nn}. Furthermore, it is well-known that rare-earth ions tend to have very small exchange energies. Consequently, as originally pointed out by Siddharthan *et al.* (*33*), magnetic dipole-dipole interactions dominate exchange in both $Ho_2Ti_2O_7$ and $Dy_2Ti_2O_7$, the opposite situation of transition metal compounds, where the dipolar forces are typically a very weak perturbation on exchange interactions. We refer to spin ice materials where magnetic dipolar interactions are the leading energy interactions as "dipolar spin ice" materials.

In order to consider the combined role of exchange and dipole-dipole interactions, it is useful to define an effective nearest-neighbor energy scale, J_{eff}, for ⟨111⟩ Ising spins:

$$J_{eff} \equiv J_{nn} + D_{nn} \qquad (3)$$

where J_{nn} is the nearest-neighbor exchange energy between ⟨111⟩ Ising moments. This simple description predicts that a ⟨111⟩ Ising system could display spin ice properties, even for antiferromagnetic nearest-neighbor exchange, $J_{nn} < 0$, so long as $J_{eff} = J_{nn} + D_{nn} > 0$. Fits to experimental data give $J_{nn} = -0.52$ K for $Ho_2Ti_2O_7$ (*28*) and $J_{nn} = -1.24$ K for $Dy_2Ti_2O_7$ (*34*). Thus, J_{eff} is positive (using $D_{nn} = 2.35$ K), hence ferromagnetic and frustrated, for both $Ho_2Ti_2O_7$ ($J_{eff} = 1.8$ K) and $Dy_2Ti_2O_7$ ($J_{eff} = 1.1$ K). It would therefore appear natural to ascribe the spin ice behavior in both $Ho_2Ti_2O_7$ and $Dy_2Ti_2O_7$ to the positive J_{eff} value as in the simple model of Bramwell and Harris (*25*). However, the situation is much more complex than it appears.

Dipole-dipole interactions are "complicated": (i) they are strongly anisotropic since they couple the spin, $\mathbf{S}_i^{\hat{z}_i}$, and space, $\mathbf{r}_{ij}$, directions, and (ii) they are also very long range ($\propto r_{ij}^{-3}$). For example, the second (next) nearest-neighbor distance is $\sqrt{3}$ times as large as the nearest-neighbor distance, and one then has a next nearest-neighbor energy scale, $D_{nnn} \approx 0.2D_{nn}$. This implies an important perturbation compared to $J_{eff} = J_{nn} + D_{nn} < D_{nn}$, especially in the context of antiferromagnetic (negative) J_{nn}. Specifically, because there are twice as many second nearest-neighbors as first nearest-neighbors in the pyrochlore lattice, for $Dy_2Ti_2O_7$, the next nearest-neighbor energy scale is about 40% of the effective nearest-neighbor energy scale . . . a large proportion! One might therefore expect that the dipolar interactions beyond nearest-neighbor would cause the different ice-rule states to have different energies, hence possibly breaking the degeneracy of the spin ice manifold. This would result in long-range Néel order with a critical temperature $T_N = O(D_{nn})$. Thus, there arises a puzzling and fascinating problem posed by the dipolar spin ice materials, that we summarize in two questions:

- Are the experimental observations of spin ice behavior consistent with dominant long-range dipolar interactions?
- If so, then why do long-range dipolar interactions fail to destroy spin ice behavior?

The minimal model one needs to consider to investigate these questions includes nearest-neighbor exchange and long-range magnetic dipole interactions:

$$H = -J\sum_{(ij)} S_i^{\hat{z}_i} \cdot S_j^{\hat{z}_j} + Dr_{nn}^3 \sum_{i>j} \frac{S_i^{\hat{z}_i} \cdot S_j^{\hat{z}_j}}{|\mathbf{r}_{ij}|^3} - \frac{3(\mathbf{S}_i^{\hat{z}_i} \cdot \mathbf{r}_{ij})(\mathbf{S}_i^{\hat{z}_i} \cdot \mathbf{r}_{ij})}{|\mathbf{r}_{ij}|^5} \qquad (4)$$

The first term is the near-neighbor exchange interaction, and the second term is the dipolar coupling between the ⟨111⟩ Ising magnetic moments. For the open pyrochlore lattice structure, we expect further neighbor exchange coupling to be very small (*35*), so it can be neglected to a good approximation. Here the spin vector $\mathbf{S}_i^{\hat{z}_i}$ labels the Ising moment of magnitude $|\mathbf{S}_i^{\hat{z}_i}| = 1$ at lattice site i and oriented along the local Ising ⟨111⟩ axis $\hat{z}_i$. The distance $|\mathbf{r}_{ij}|$ is measured in units of the nearest-neighbor distance, r_{nn}. J represents the exchange energy and $D = (\mu_0/4\pi)\mu^2/r_{nn}^3$. Because of the local Ising axes, the effective nearest-neighbor energy scales are $J_{nn} \equiv J/3$ and, as mentioned above, $D_{nn} \equiv 5D/3$, since $\hat{z}_i \cdot \hat{z}_j = -1/3$ and $(\hat{z}_i \cdot \mathbf{r}_{ij})(\mathbf{r}_{ij} \cdot \hat{z}_j) = -2/3$. If $D_{nn} = 0$ one obtains the spin ice model originally proposed by Harris and colleagues (*15*, *25*), henceforth referred to as the "near-neighbor spin ice model."

Siddharthan *et al.* (*33*) first addressed the role of dipole-dipole interactions in Ising pyrochlore materials, both $Dy_2Ti_2O_7$ (*29*) and $Ho_2Ti_2O_7$ (*33*, *36*). They considered Eq. 4 above, but restricted the dipolar lattice sum up to the first 5 nearest neighbors (*33*), or 10 and 12 nearest neighbors (*36*). With the values they used for J_{nn} and D_{nn} the conclusion that they reached was that a spin ice state could exist for their model of $Dy_2Ti_2O_7$ but not for their model of $Ho_2Ti_2O_7$, where a partially ordered state was predicted. It was suggested that a transition to this partially ordered state was consistent with a sharp rise in the experimental specific heat of $Ho_2Ti_2O_7$ observed below ~1 K (*33*). The reported specific-heat rise has more recently been shown to be consistent with the freezing of the nuclear spins of ^{165}Ho, as discussed below. However, the results of reference (*33*) did appear to give a negative answer to the first of the above questions: The dipolar model, it seemed, was inconsistent with the experimental data that supported a disordered spin ice ground state for $Ho_2Ti_2O_7$ (*15*).

On the other hand, direct dipolar lattice sums are notoriously tricky to handle, and truncation of dipolar interactions at some arbitrarily chosen fixed finite distance often gives rise to spurious results. One approach that has been successfully used to obtain reliable quantitative results for real dipolar materials (*37*) is the Ewald summation method (*38*, *39*). This method is conceptually akin to the well-known Madelung approach used to calculate electrostatic Coulomb energies in ionic crystals. The Ewald summation method generates an absolutely convergent effective dipole-dipole interaction between two spins i and j. This is done by periodically replicating a specified volume and summing convergently the interactions between i and j and all the periodically repeated images of j. Once an effective dipole-dipole interaction between spins i and j within the simulation cell has been derived via the Ewald summation technique, one can perform Monte Carlo simulations using the standard Metropolis algorithm. This technique was applied to the dipolar spin ice model by den Hertog and Gingras (*34*), who found, contrary to the results of references (*33*) and (*36*), no sign of full or partial ordering for all $J_{eff}/D_{nn} \geq 0.09$. The system was characterized as having spin-ice behavior by determining the entropy, via numerical integration of $C(T)/T$. For $J_{eff}/D_{nn} \geq 0.09$, the recovered magnetic entropy was found to be within a few percent of Pauling's value $R[\ln(2) - (1/2)\ln(3/2)]$ (*34*). It was shown in reference (*34*) that the only free parameter in the theory is J_{nn}, which can be determined by comparing the experimental and theoretical specific-heat temperature peak T_{peak} referred to above. This procedure gives $J_{nn} = -1.24$ K for $Dy_2Ti_2O_7$ (*34*) and $J_{nn} = -0.52$ K for $Ho_2Ti_2O_7$ (*28*). Figure 3 shows the very good agreement obtained from Monte Carlo simulations results, using Ewald summation methods (*34*), with the experimental results for $Dy_2Ti_2O_7$ (*29*). These numerical results give a definite answer to at least the first of the two questions posed above: Dominant long-range dipolar interactions are indeed consistent with the spin ice behavior observed in the dipolar spin ice materials (*40*). We find it remarkable that long-range dipolar coupling can, through some effective self-screening, restore the ice-rules degeneracy to such a striking degree (*41*). Consequently, we feel that the second question—the "why?"—has not yet been answered in any simple and definite way.

In order to further test the proposal that

the formation of the spin ice state in real materials is due to long-range dipole-dipole interactions, one needs to compare the spin-spin correlations in real systems with that predicted by the dipolar spin ice model. Recently, elastic neutron-scattering experiments on a flux-grown single crystal of $Ho_2Ti_2O_7$ have found excellent agreement with the predictions of the dipolar spin ice model, and they establish unambiguously the spin ice nature of the zero-field spin correlations in that material (*28*). These results also show that the dipolar interactions beyond nearest neighbor do slightly favor some of the spin ice states over others although they do not significantly affect the ground state entropy.

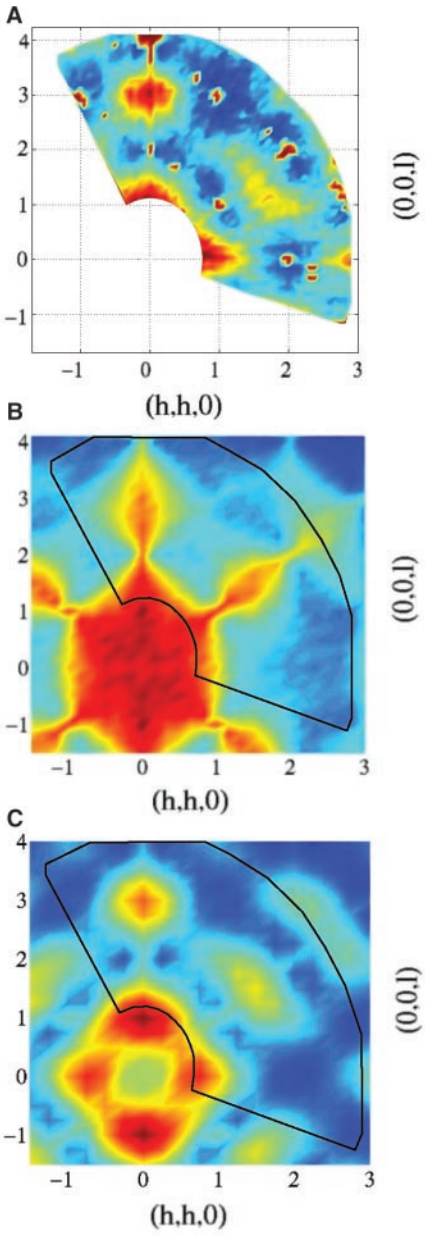

Fig. 4. (**A**) Experimental neutron-scattering pattern of $Ho_2Ti_2O_7$ in the (*hhl*) plane of reciprocal space at $T \approx 50$ mK (*28*). Dark blue shows the lowest intensity level, red-brown the highest. Temperature-dependent measurements have shown that the sharp diffraction spots in the experimental pattern are nuclear Bragg peaks with no magnetic component. (**B**) Calculated neutron scattering for the nearest-neighbor spin ice model at $T = 0.15J$. (**C**) Calculated neutron scattering for the dipolar spin ice model at $T = 0.6$ K. This can be compared with the experimental scattering because the latter is temperature-independent in this range. The areas defined by the solid lines denote the experimental data region of (A).

The elastic neutron-scattering pattern of $Ho_2Ti_2O_7$ at $T \sim 50$ mK is shown in Fig. 4 and compared with theoretical predictions for the near-neighbor and dipolar spin ice models. The pattern for near-neighbor spin ice successfully reproduces the main features of the experimental pattern, but there are important differences, both qualitative and quantitative, notably in the extension of the 0, 0, 0 intense region along [*hhh*] and the relative intensities of the regions around 0, 0, 3 and 3/2, 3/2, 3/2. Also, the experimental data show much broader regions of scattering along the diagonal directions. The dipolar model successfully accounts for these discrepancies. In particular, it predicts the four intense regions around 0, 0, 0, the relative intensities of the regions around 0, 0, 3 and 3/2, 3/2, 3/2, and the spread of the broad features along the diagonal. The neutron-scattering data can in fact be accurately and quantitatively accounted for by the dipolar model with no free parameter, once J_{nn} has been determined by the height of the specific-heat peak (*28*). Qualitatively similar scattering has been observed in water ice and described by an ice-rules configuration of protons (*8*).

To complete the description of the static properties of $Ho_2Ti_2O_7$, it was shown in reference (*28*) that the specific heat could be very accurately described by the sum of the dipolar spin ice contribution, with $D_{nn} = 2.35$ K, $J_{nn} = -0.52$ K, and a nuclear spin contribution with level splitting at ~0.3 K, the large value typical of a Ho^{3+} salt. Analysis of the hyperfine contribution followed the early work of Blöte *et al.* (*17*), who observed that the specific heat of isostructural Ho_2GaSbO_7 can be accurately fitted by the sum of two Schottky contributions, one arising from the nuclear and one from the electronic spins. It is interesting to note that these authors had also commented on some evidence for a residual entropy in $Dy_2Ti_2O_7$, later attributed by Ramirez *et al.* to spin ice behavior (*29*).

The above results show that dipole-dipole interactions can cause spin ice behavior, and that the simple spin Hamiltonian defined in Eq. 4 can provide a quantitative description of experimental results on real materials. In the next section, we discuss how, if dynamics can be preserved in simulations, that dipole-dipole interactions do stabilize a long-range Néel order at a critical temperature $T_c \ll D_{nn}$, hence partially addressing the second question above.

Open Issues and Avenues for Future Research

Among open issues in the physics of dipolar spin ice materials are the question of the "true ground state," the magnetic field–dependent behavior, the effect of diamagnetic dilution, the nature of the spin dynamics, and the properties of spin ice–related materials.

The question of a true ground state has long intrigued researchers on water ice, and the same question applies to spin ice. A common interpretation of the third law of thermodynamics is that the true ground state of a real system must be ordered, without entropy. If the system is ergodic, that is, it can explore all its possible arrangements, then presumably it should settle into its absolutely minimum energy ground state, which we refer to as its "true" ground state. This is not observed, either in water ice or in the spin ice materials. However, the experimental zero-point entropy does not necessarily mean that the system does explore its spin ice manifold on the time scale of the experiment. Rather, it suggests that the system, with a finite correlation length, is self-averaging, so the thermodynamic average over one state is equivalent to the canonical average over an ensemble of states (*42*). If the system is "stuck" in a disordered state, then, as discussed in the last section, the following question arises: Would the long-range part of dipolar interaction stabilize a true ground state of lower energy than all the other spin ice states if it was not dynamically inhibited from forming as the system is cooled through the temperature $T \sim J_{eff}$ at which the ice-rule manifold develops? Recent theoretical work on the dipolar spin ice model has answered the above question in the affirmative: The low-energy frozen state that forms does indeed depend on the dynamics introduced (*43*). Numerical simulation of the dipolar spin ice model

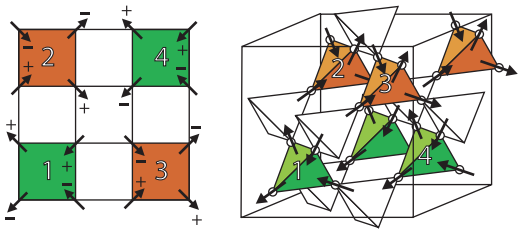

Fig. 5. The predicted long-range ordered state of dipolar spin ice. Projected down the *z* axis (**A**), the four tetrahedra making up the cubic unit cell appear as dark gray squares. The light gray square in the middle does not represent a tetrahedron; however, its diagonally opposing spins occur in the same plane. The component of each spin parallel to the *z* axis is indicated by a plus and minus sign. In perspective (**B**), the four tetrahedra of the unit cell are numbered to enable comparison with (A).

with single spin flips gives a disordered ground state as observed in experiment (*15*, *30*, *31*), but the introduction of "loop moves," that is, correlated flipping of extended groups of spins (Fig. 1C), gives rise to a first order transition to an ordered state. The transition is predicted to be independent of J_{nn}, with $T_c \approx 0.077 D_{nn} \approx 0.18$ K for both $Ho_2Ti_2O_7$ and $Dy_2Ti_2O_7$ (*43*). The ordered state is illustrated in Fig. 5. It corresponds to a tetrahedral two-in, two-out basis of spins, inverted by two out of the three face-centering translations in the unit cell. It is interesting that a structure of related symmetry (the "$Q = X$" phase) has been observed in $Ho_2Ti_2O_7$ after the application of a field, as discussed below. An intriguing possibility is that the predicted ordered state might be accessible by a suitable field and temperature cycle in the spin ice regime. The theoretical ordered state identified in (*43*) is compatible with the critical (soft) mode identified in a mean-field theory treatment of the dipolar spin ice model (*31*, *41*). It would appear possible that it is the true ground state of the real materials, as the Ewald method of (*34*, *43*) gives the correct quantitative description of experiment in regard to the paramagnetic disordered spin ice state. However, references (*33*) and (*36*) argue that it is the truncation method, rather than the Ewald method, that gives the true ground state of the dipolar model, suggesting that the mathematical problem of determining the true ground state is not yet resolved (*40*).

The zero-field static properties of the spin ice materials $Ho_2Ti_2O_7$ (*28*) and $Dy_2Ti_2O_7$ (*29*, *34*) and most recently $Ho_2Sn_2O_7$ (*31*) can now be considered to be very well described by the dipolar spin ice model. The essential scenario is a continuous freezing process into a disordered magnetic state below ~1 K. In the earliest study of $Ho_2Ti_2O_7$, it was pointed out that its field-dependent static properties were far from trivial (*15*). Two ordered magnetic phases were observed to develop rapidly in a magnetic field of ~0.1 T applied along [1$\bar{1}$0] at base temperature of ~50 mK. Both of these can be described with the same tetrahedral basis as the face-centered cubic crystal structure, but one has "ferromagnetic" face centering, the $Q = 0$ phase, and the other has partial "antiferromagnetic" face centering, the $Q = X$ phase. It has been shown that both states fulfill the spin ice rules (*15*). The field-induced order displays a strong dependence on the exact experimental warming or cooling procedure followed (so-called "history dependence") for field up to 3 T and temperature from 50 mK to 2 K. Low-temperature susceptibility studies, discussed below, have confirmed that a strongly history-dependent magnetic moment can be induced by an applied field below a temperature of ~0.7 K (*44*) (Fig. 6). Theoretical studies of the near-neighbor spin ice model (*27*) suggest several interesting effects as the field is applied along the other main symmetry directions, [100] and [111]. Application of a field along [100] breaks symmetry such that each tetrahedron has the same two-in, two-out state, but a symmetry sustaining first-order phase transition is predicted, analogous to the liquid-gas transition or those that can be observed in ferroelectrics (*27*, *45*). A field of several Tesla along [111] breaks the ice rules to give a state with three in and one out (or vice versa). This transition, also predicted by the dipolar model (*46*), has been observed by single-crystal magnetization measurements at 2*K*, first on $Ho_2Ti_2O_7$ by Cornelius and Gardner (*22*) and more recently on $Dy_2Ti_2O_7$ by Fukazawa *et al.* (*47*). These two studies reveal a potentially interesting difference between the two compounds: Although the saturation magnetization of $Dy_2Ti_2O_7$ along the three main symmetry directions is in remarkable quantitative agreement with the predictions of the spin ice rules (*47*), that for $Ho_2Ti_2O_7$ shows a significant departure (*22*). At 2*K* the field-dependent behavior of the spin ice materials appears to be equally well described by the dipolar and near-neighbor models. However, it is most unlikely that the success of the oversimplified near-neighbor model will extend to lower temperatures. Hints of this have already been observed in the specific heat of $Dy_2Ti_2O_7$, where polycrystalline samples display several thermal anomalies, as a function of field and temperature, that do not agree with the near-neighbor model (*29*). It would be hoped that the dipolar spin ice model will account for these details (*46*). The field-dependent and related field–induced relaxational dynamic behavior of spin ice materials promises to be an interesting area of research. For example, recent neutron studies show that the magnetization process in the spin ice regime of a single crystal sample of $Dy_2Ti_2O_7$ occurs via a series of steps and plateaus (*30*).

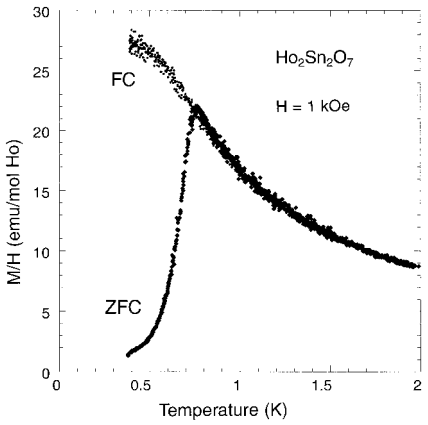

Fig. 6. Temperature dependence of the dc magnetization of the $Ho_2Sn_2O_7$ spin ice material in an applied magnetic field, *H*, of 1 kOe [from (*44*)]. Zero-field cooled, ZFC, denotes a procedure that involves cooling in zero field and measuring the magnetization, *M*, upon warming with the field *H* on. Field cooled, FC, involves cooling the sample in a field, *H*, and measuring the magnetization, *M*, with the field on.

The dynamics of the Ising spins in spin ice materials is of broad potential interest in context of the long-standing problem of the proton dynamics in the various phases of water ice (*48*). Matsuhira *et al.* have investigated the dynamic properties of the spin ice materials $Ho_2Ti_2O_7$ and $Ho_2Sn_2O_7$ by measuring both direct current (dc) and alternating current (ac) magnetization (*44*). History dependence of the dc magnetization in the spin ice phase shows a sharp splitting between field-cooled and zero field–cooled susceptibility, indicative of the expected spin freezing process (Fig. 6). The characteristic response of the ac magnetization is peaked near ~1 K, which shifts to higher temperature with increasing frequency. This can be analyzed in terms of an thermally activated Arrhenius-type spin relaxation with a characteristic relaxation time of $\sim 10^{-10}$ s and an activation barrier of 28 K and 20 K for $Ho_2Ti_2O_7$ and $Ho_2Sn_2O_7$, respectively. This behavior may be compared with that of other types of magnetic system that exhibit spin freezing (*49*). In fine-particle magnets, one observes the thermally activated flipping of independent spin clusters, which becomes frozen, or "blocked," at low temperature, whereas in certain dilute transition metal alloys (such as $AuFe_{0.01}$), one observes "spin glass" behavior in which the spin freezing is a cooperative process. The behavior of $Ho_2Ti_2O_7$ and $Ho_2Sn_2O_7$ appears more similar to a blocking phenomenon than to a spin glass transition (*44*). Very recently, two ac-magnetization studies of $Dy_2Ti_2O_7$ have been reported (*50*, *51*). The first of these studies, by Matsuhira *et al.* (*50*) finds behavior below 2 K analogous to that of $Ho_2Ti_2O_7$ and $Ho_2Sn_2O_7$, which, if fitted to an Arrhenius expression gives an activation barrier of 10 K. This process is cautiously ascribed to spin ice freezing. In addition, Matsuhira *et al.* report an ac susceptibility peak that is observed above 10 K, which indicates an Arrhenius-type response with a large activation energy of 220 K. This high-temperature susceptibility peak is also observed in the second study, by Snyder *et al.* (*51*). However, the two reports disagree in their interpretation of this feature. Snyder *et al.* argue that the high-temperature susceptibility peak reflects a single relaxation time and ascribe this to spin ice freezing. Matsuhira *et al.*, in contrast, suggest that the high-temperature susceptibility peak indicates a spread of relaxation times, at least near to $T \sim 10$ K, but do not speculate on the physical origin. It would be premature to discuss which interpretation might be correct, but it would seem to us that in view of the energy scale, another possible physical origin worth investigating is spin-lattice relaxation. The dynamics of spin ice materials is clearly an active area of research. We also note μSR studies on $Ho_2Ti_2O_7$ (*23*) and theoretical investigations into ordered state selection in spin ice models via quantum fluctuations, as ongoing research activities (*52*).

Possible modifications of spin ice materials

include doping with diamagnetic impurities. In water ice, doping with KOH (which effectively removes protons) leads to the ordered phase known as ice XI (*53*): It is believed that the holes introduced in the proton structure "free up" the dynamics so that the system can find its true ordered ground state. In the case of spin ice it is not clear that dilution with diamagnetic impurities, such as replacing Ho^{3+} and Dy^{3+} by nonmagnetic Y^{3+}, will have the same effect (*46*). However, dilution is likely to have some effect on the dynamical properties on the spin ice state. With considerable dilution, one would expect to form a spin glass state. Such studies might go a long way to clarifying the precise differences between the spin ice state and the spin glass state, and their similarities, or lack thereof, in their freezing mechanisms. The fact that spin ice is "self-averaging" (see above), whereas a spin glass is not (*49*), points to the essentially simpler nature of the spin ice–freezing process. However it is not yet clear how such a detailed difference will manifest itself experimentally.

Perhaps the most fruitful area of future research will be into materials and models which can be considered derived from or related to spin ice. At a theoretical level the near-neighbor spin ice model of (*25*) is a "16-vertex" model of the ferroelectric type long studied by theoreticians (*13*); the discovery of spin ice materials is giving a new experimental relevance to these models (*54*, *55*). Modifications of the near-neighbor model may be designed to include quantum mechanical effects (*52*) or the effect of finite anisotropy (*56*). Such models might be relevant to as-yet-undiscovered spin ice materials based on transition metal ions, where spin values are smaller and exchange is larger. Known spin ice–related materials include the frustrated pyrochlore magnet $Tb_2Ti_2O_7$, the behavior of which remains essentially mysterious (*57*, *58*). $Tb_2Ti_2O_7$ has been described as a "cooperative paramagnet" (*57*), but it may also share some properties with the spin ice materials (*34*, *58*). Another example is $Nd_2Mo_2O_7$, in which spin ice–like correlations on the Nd sublattice perturb the metallic behavior on the Mo sublattice to give a striking anomalous Hall effect (*59*). A final example is $Dy_2Ir_2O_7$, a metallic material, but in which the Dy spins appear to be antiferromagnetically coupled, leading to an ordering transition (*60*). The possibility that one could obtain a metallic spin ice is an intriguing one: The conduction electron–mediated coupling of localized spins, the so-called Ruderman-Kittel-Kasuya-Yosida (RKKY) interaction, is similarly long-ranged to the dipolar interaction. Perhaps this long-range coupling could, as does the dipolar interaction, stabilize spin ice behavior. If so, it would represent another novel realization of the concept of spin ice.

In conclusion, the previous discussion emphasizes the current interest in systems in which the strong magnetic anisotropy of localized *f* electrons leads to novel collective effects based on frustration. The spin ice phenomenon exemplifies the richness of the intrinsic physics of frustration while, at the same time, affording a close connection between theory and experiment. This has allowed real progress to be made and some surprising properties (for example, the effective self-screening of the long-range dipolar interactions) to be identified. One may hope that the current experimental and theoretical studies of spin ice materials will lead to a deeper understanding of the effects of frustration in related rare-earth (*59*, *61*, *62*) and transition metal magnets. This in turn should provide a solid platform from which we can consolidate our understanding of the diverse electronic phenomena in which frustration is, or might be, implicated. Exciting topical examples include heavy-fermion behavior in LiV_2O_4 (*63*, *64*), spin-Peierls–related phenomenon in $ZnCr_2O_4$ (*65*), and superconductivity in $Cd_2Re_2O_7$ (*66*–*68*). We expect that new collective phenomena in spin ice materials and their relatives will continue to capture the attention of condensed-matter physicists and solid-state chemists for years to come.

References and Notes

1. G. Toulouse, *Commun. Phys.* **2**, 115 (1977).
2. W. F. Giauque, M. F. Ashley, *Phys. Rev.* **43**, 81 (1933).
3. W. F. Giauque, J. W. Stout, *J. Am. Chem. Soc.* **58**, 1144 (1936).
4. L. Pauling, *J. Am. Chem. Soc.* **57**, 2680 (1935).
5. D. Bernal, R. H. Fowler, *J. Chem. Phys.* **1**, 515 (1933).
6. J. F. Nagle, *J. Math. Phys.* **7**, 1484 (1966).
7. E. O. Wollan *et al.*, *Phys. Rev.* **75** 1348 (1949).
8. J. C. Li *et al.*, *Philos. Mag. B* **69**, 1173 (1994).
9. H. T. Diep, Ed. *Magnetic Systems with Competing Interactions* (World Scientific, Singapore, 1994).
10. P. Schiffer, A. P. Ramirez, *Comm. Condens. Matter Phys.* **18**, 21 (1996).
11. J. E. Greedan, *J. Mater. Chem.* **11**, 37 (2001).
12. R. J. Baxter, *Exactly Solved Models in Statistical Mechanics* (Academic Press, New York, 1982).
13. E. H. Lieb, F. Y. Wu, *Phase Transitions and Critical Phenomena*, C. Domb and M. S. Green, Eds. (Academic Press, New York, 1972), pp. 332–490.
14. P. W. Anderson, *Phys. Rev.* **102**, 1008 (1956).
15. M. J. Harris, S. T. Bramwell, D. F. McMorrow, T. Zeiske K. W. Godfrey, *Phys. Rev. Lett.* **79**, 2554 (1997).
16. The crystal was grown by K. W. Godfrey, Clarendon Laboratory, Oxford.
17. H. W. J. Blöte *et al.*, *Physica* **43**, 549 (1969).
18. L. G. Mamsurova *et al.*, *Sov. Phys. Solid State* **27**, 1214 (1985).
19. S. T. Bramwell, M. N. Field, M. J. Harris I. P. Parkin, *J. Phys. Condens. Matter* **12**, 483 (2000).
20. Y. M. Jana, D. Ghosh, *Phys. Rev. B* **61**, 9657 (2000).
21. S. Rosenkranz *et al.*, *J. Appl. Phys.* **87**, 5914 (2000).
22. A. L. Cornelius, J. S. Gardner, *Phys. Rev. B* **64**, 060406 (2001).
23. M. J. Harris, S. T. Bramwell, T. Zeiske, D. F. McMorrow, P. J. C. King, *J. Magn. Magn. Mater.* **177**, 757 (1998).
24. J. D. Cashion *et al.*, *J. Mater. Sci.* **3**, 402 (1968).
25. S. T. Bramwell, M. J. Harris, *J. Phys. Condens. Matter* **10**, L215 (1998).
26. R. Moessner, *Phys. Rev. B* **57**, R5587 (1998).
27. M. J. Harris, S. T. Bramwell, P. C. W. Holdsworth, J. D. M. Champion, *Phys. Rev. Lett.* **81**, 4496 (1998).
28. S. T. Bramwell *et al.*, *Phys. Rev. Lett.* **87**, 047205 (2001).
29. A. P. Ramirez *et al.*, *Nature* **399**, 333 (1999).
30. T. Fennell *et al.*, http://xxx.lanl.gov/abs/cond-mat/0107414.
31. H. Kadowaki, Y. Ishii, K. Matsuhira, Y. Hinatsu, http://xxx.lanl.gov/abs/cond-mat/0107278.
32. M. Harris, *Nature*, **399**, 311 (1999).
33. R. Siddharthan *et al.*, *Phys. Rev. Lett.* **83**, 1854 (1999).
34. B. C. den Hertog, M. J. P. Gingras, *Phys. Rev. Lett.* **84**, 3430 (2000).
35. J. E. Greedan *et al.*, *Chem. Mater.* **10**, 3058 (1998).
36. R. Siddharthan, B. S. Shastry, A. P. Ramirez, *Phys. Rev. B* **63**, 184412 (2001).
37. See, for example, comparison between experiment and theory for the dipolar diamond lattice: S. J. White *et al.*, *Phys. Rev. Lett.* **71**, 3553 (1993).
38. J. M. Ziman, *Principles of the Theory of Solids* (Cambridge Univ. Press, Cambridge, ed. 2, 1972).
39. M. Born, S. Huang, *Dynamical Theory of Crystal Lattices* (Oxford Univ. Press, New York, 1968).
40. We believe that the Ewald method is the correct approach to treating the dipolar interactions, especially in view of the fact that it gives excellent agreement with experiment (*28*). Siddharthan *et al.* have argued in references (*33*) and (*36*) that truncation, rather than the Ewald method, is the correct approach but they do not comment on the conflict that this creates with experiment. For the time being, this remains something of a controversy that needs further investigation.
41. M. J. P. Gingras, B. C. den Hertog, http://xxx.lanl.gov/abs/cond-mat/0012275; *Can. J. Phys.*, in press.
42. We thank P. Holdsworth for a discussion on this point.
43. R. G. Melko, B. C. den Hertog, M. J. P. Gingras, *Phys. Rev. Lett.* **87** 067203 (2001).
44. K. Matsuhira, Y. Hinatsu, K. Tenya, T. Sakakibara, *J. Phys. Condens. Matter* **12**, L649 (2000).
45. T. Mitsui *et al.*, *An Introduction to the Physics of Ferroelectrics*, *Ferroelectricity, and Related Phenomena*, vol. 1, I. Lefkowitz and G. I. Taylor, Eds. (Gordon & Breach, London, 1986).
46. R. G. Melko, thesis, University of Waterloo, Ontario, Canada (2001).
47. H. Fukazawa, R. G. Melko, R. Higashinaka, Y. Maeno, M. J. P. Gingras, http://xxx.lanl.gov/abs/cond-mat/0108129.
48. V. F. Petrenko, R. W. Whitworth, *Physics of Ice* (Oxford Univ. Press, Oxford, 1999).
49. J. A. Mydosh, *Spin Glasses, an Experimental Introduction* (Taylor & Francis, London and Washington, DC, 1993).
50. K. Matsuhira, Y. Hinatsu, T. Sakakibara, *J. Phys. Condens. Matter* **13,** L737 (2001).
51. J. Snyder, J. S. Slusky, R. J. Cava, P. Schiffer, *Nature* **413** 48 (2001).
52. R. Moessner, O. Tchernyshyov, S. L. Sondhi, cond-mat/0106286.
53. Y. Tajima, T. Matsuo, H. Suga, *Nature* **299**, 810 (1982).
54. G. I. Watson, *J. Stat. Phys.* **94**, 1045 (1999).
55. A. J. Garcia-Adeva, D. L. Huber, *Phys. Rev. B*, **64** 014418 (2001).
56. J. D. M. Champion, S. T. Bramwell, P. C. W. Holdsworth, M. J. Harris, http://xxx.lanl.gov/abs/cond-mat/0103051.
57. J. S. Gardner *et al.*, *Phys. Rev. Lett.* **82**, 1012 (1999).
58. M. J. P. Gingras *et al.*, *Phys. Rev. B* **62**, 6496 (2000).
59. Y. Taguchi, Y. Oohara, H. Yoshizawa, N. Nagaosa, Y. Tokura, *Science* **291**, 2573 (2001).
60. D. Yanagishima, Y. Maeno, http://xxx.lanl.gov/abs/cond-mat/0106330.
61. J. D. M. Champion *et al.*, *Phys. Rev. B* **64**, 140407(R) (2001).
62. S. E. Palmer, J. T. Chalker, *Phys. Rev. B* **62**, 488 (2000).
63. S. Kondo *et al.*, *Phys. Rev. Lett.* **78**, 3729 (1997).
64. S.-H. Lee, Y. Qiu, C. Broholm, Y. Ueda, J. J. Rush, *Phys. Rev. Lett.* **86**, 5554 (2001), and references therein.
65. S.-H. Lee, C. Broholm, T. H. Kim, W. Ratcliff, S. W. Cheong, *Phys. Rev. Lett.* **84**, 3718 (2000).
66. R. Jin *et al.*, *Phys. Rev. B* **64**, R15138 (2001).
67. M. Hanawa *et al.*, *Phys. Rev. Lett.* **87**, 187001 (2001).
68. H. Sakai *et al.*, *J. Phys. Condens. Matter* **13**, L785 (2001).

69. It is a pleasure to thank our present collaborators for their contribution to some of the ideas expressed here: D. Champion, B. den Hertog, S. Dunsiger, B. Fåk, T. Fennell, J. Gardner, P. Holdsworth, R. Kiefl, J. Lago, R. Melko, O. Petrenko and A. Wills. We thank R. Melko for his help with the figures. We acknowledge stimulating discussions with P. Schiffer, Y. Maeno, and K. Matsuhira. M.G. acknowledges financial support from NSERC of Canada, Research Corporation, and the Province of Ontario. S.T.B. would like to express particular thanks to M. Harris for their long-standing collaboration in this field.

Spin Ice State in Frustrated Magnetic Pyrochlore Materials

Steven T. Bramwell and Michel J. P. Gingras

Science **294**, 1495 (2001);
DOI: 10.1126/science.1064761

Science (print ISSN 0036-8075; online ISSN 1095-9203) is published weekly, except the last week in December, by the American Association for the Advancement of Science, 1200 New York Avenue NW, Washington, DC 20005.